International Journal of Climatology

International Journal of Climatology RMetS

RESEARCH ARTICLE

An Elevated Influence of the Low-Latitude Drivers on the East Asian Winter Monsoon After Around 1990

Bozhou Chen[1] | Keyan Fang[2] | Zepeng Mei[2] | Tinghai Ou[3] | Feifei Zhou[2] | Hao Wu[2,4] | Zheng Zhao[2] | Deliang Chen[3,5]

[1]Zijin School of Geology and Mining, Fuzhou University, Fuzhou, China | [2]Key Laboratory of Humid Subtropical Eco-Geographical Process (Ministry of Education), Fujian Normal University, Fuzhou, China | [3]Regional Climate Group, Department of Earth Sciences, University of Gothenburg, Gothenburg, Sweden | [4]State Key Laboratory of Nuclear Resources and Environment, East China University of Technology, Nanchang, Jiangxi, China | [5]Department of Earth System Sciences, Tsinghua University, Beijing, China

Correspondence: Keyan Fang (kfang@fjnu.edu.cn)

Received: 7 May 2024 | **Revised:** 23 October 2024 | **Accepted:** 25 October 2024

Funding: This study was supported by the National Natural Science Foundation of China (42101082 and 42130507), China Postdoctoral Science Foundation (2023M730602).

Keywords: Arctic oscillation | east Asian winter monsoon | westerlies | Western Pacific

ABSTRACT

Current East Asian winter monsoon (EAWM) indices effectively depict the associated high- and low-latitude atmospheric circulations. However, the spatial dynamics of the winter coldness within the monsoon domain are not well adequately represented by EAWM indices. We introduce a novel approach to classify winter temperatures based on both their co-variability and their mean values. We classified the EAWM domain into three distinct modes: northern (ranging from −27°C to −15°C), central (−14°C to 5°C), and southern (6°C to 27°C). The northern mode, characterised by intense coldness, correlates with a strengthened westerlies that traps Arctic cold air masses during the positive phase of the Arctic Oscillation (AO). In contrast, the southern mode is primarily influenced by low-latitude oceanic and atmospheric patterns, particularly for near-coast areas. The central mode, representing an interplay of both high and low-latitude processes, encapsulates the comprehensive characteristics of the EAWM. Our analysis reveals a notable shift in the relationships among the northern, central, and southern modes around 1990. Prior to this year, the EAWM was predominantly influenced by northern atmospheric patterns, while there is a discernible increase in the influence of low-latitude drivers afterwards. This shift may be linked to the significant warming in the western Pacific and Indian Oceans, underscoring the heightened role of low-latitude drivers on the EAWM.

1 | Introduction

The East Asian winter monsoon (EAWM) represents the most robust winter circulation system in the Northern Hemisphere, exerting a profound impact on the climate from high to tropical Asia (Duan, Zhang, and Lv 2013; Jin et al. 2019; Wang et al. 2006; Wang and Lu 2017). Linked with extreme coldness and significant snowpack, the EAWM often leads to substantial socioeconomic losses, disrupting everyday life, including traffic, tourism, and agriculture (Duan, Zhang, and Lv 2013; Li et al. 2023). For example, the large-scale low temperatures, rain, snow, and freezing conditions in China from January to February 2008, the East Asian cold wave in January 2021, and the cold wave in 2022 were all influenced by the EAWM, causing direct economic losses of 151.6 billion yuan, 6.63 billion yuan, and 7.89 billion yuan, respectively (Li et al. 2023; Tao and Wei 2008; Yu et al. 2022).

The EAWM is primarily driven by the Siberian-Mongolian High, under the significant influence of the Arctic cold air mass, closely associated with the Arctic Oscillation (AO) (Gong, Wang, and Zhu 2001). Concurrently, the low-pressure systems over the maritime continent in the low latitudes also significantly modulate the EAWM towards the tropics (Huang, Wang, and Wright 2016; Jhun and Lee 2004; Liu et al. 2012). Various EAWM indices have been proposed to capture its dynamic patterns (Liu et al. 2012; Wang and Chen 2010), including the pressures of the Siberian-Mongolian High (Wang et al. 2006), its contrast with oceanic and low-latitude pressures (Li and Yang 2010), surface northerlies (Yang, Lau, and Kim 2002), upper-level jet streams (Jhun and Lee 2004), and potential vorticity (Huang, Wang, and Wright 2016). The EAWM predominantly influences temperature reductions in East Asia (Wang et al. 2006), contrasting the EASM's primary impact on precipitation (Huang et al. 2023; Wang et al. 2013). Consequently, EAWM indices often incorporate mean temperature anomalies across the entire monsoon domain (Lee et al. 2013). However, there are ongoing debates regarding the ability of these indices to effectively characterise temperature and precipitation anomalies in the East Asian monsoon region. Some studies (Wang and Chen 2010) have pointed out that these indices fail to accurately capture the main features of winter temperature variations in China, as they are primarily based on a single EAWM circulation component and are influenced by the region's complex underlying topography (Ao et al. 2024). This limitation hinders our understanding of the dynamic influences of high- and low-latitude drivers on the EAWM.

To address this knowledge gap, we utilise the covarying isoline method, which effectively delineates areas encircled by climatic isolines, such as those for precipitation or temperature (Fang et al. 2024). This approach aligns well with our objective to map large-scale covarying winter temperature isolines within the monsoon domain and investigate their regimes associated with high- and low-latitudes drivers. According to Liu et al. (2012), the East Asian low-latitude winter monsoon (EAWM-L) and mid-high-latitude winter monsoon (EAWM-M) indices are defined by the 1000 hPa meridional wind (v wind) averaged over the regions (10° N–25° N, 105° E–135° E) and (30° N–50° N, 110° E–125° E), respectively (Liu et al. 2012). We selected the broader East Asian winter monsoon region (10° N–50° N, 105° E–135° E), which encompasses both the high- and low-latitude components, enabling a comprehensive analysis of the factors influencing the monsoon across different latitudes.

2 | Data Sources and Research Methods

2.1 | Climate Data

In this research, we utilised the Climate Research Unit (CRU TS4.07) temperature dataset, which provides monthly resolution data in a 0.5° × 0.5° grid system, covering the period from 1901 to 2022 (Harris et al. 2020). Given that the majority of meteorological stations in Central and Eastern Asia, contributing to this dataset, were established post-1950, we specifically focused on temperature data from this period onwards (Cook et al. 2010). To understand the interaction between temperature and oceanic-atmospheric conditions, we examined correlations with sea surface temperature (SST), geopotential height (GPH), and near-surface wind speed. For SST, we employed the HadISST dataset from the Met Office Hadley Centre for Climate Prediction and Research, offering 1° × 1° spatial resolution and extending from 1870 to the present (Rayner et al. 2003). GPH and wind data were sourced from the European Center for medium-range weather forecasting (ECMWF) Reanalysis version 5 (ERA5), providing a finer spatial resolution of 0.25° × 0.25°, and ranging from 1950 to present (Hersbach et al. 2023). The AO was first introduced by Thompson and Wallace (1998). It is typically defined as the leading mode of the empirical orthogonal function (EOF) decomposition of sea level pressure fields north of 20° N. The AO index used in this study is sourced from https://www.cpc.ncep.noaa.gov/products/precip/CWlink/daily_ao_index/ao.shtml.

2.2 | Analytical Methods

Our approach hinges on the concept of the covarying isoline method, which interprets the monsoon as a seasonal temperature shift from high to low latitudes, driven by large-scale circulation patterns (Liu et al. 2012). A specific monsoon-associated circulation pattern is expected to cause a set of temperature isolines to exhibit covarying trends. To this end, we first calculated the areas below temperature isolines ranging from −27°C to 27°C in 1°C increments within the EAWM domain for the winter season (December–February) since 1950. These areas were weighted using the Cylindrical Equal Area projection method to account for geographic distortion (Snyder 1987). Temperature isolines were then grouped based on their inter-correlations using hierarchical clustering analysis, with a threshold set at 30% of the maximum distance (Ward 1963).

Pearson correlation analysis was used to calculate the relationships between variables. The wavelet coherence (WTC) (Grinsted, Moore, and Jevrejeva 2004) was used to assess time-dependent correlations between the areas below specific temperature isolines. This technique decomposes time series data into different temporal components through wavelet analysis, followed by calculating localised correlations across various scales. Additionally, running correlations with a 21-year window were utilised to detect dynamic relationships among the areas below different temperature isolines, providing insights into their temporal evolution.

3 | Results

We revealed distinct modes of EAWM temperatures corresponding to the northern (below −27°C to −15°C), central (below −14°C to 5°C), and southern (below 6°C to 27°C) modes (Figure 1a). These modes are geographically demarcated with the northern mode primarily above 45° N, the central mode encompassing areas north of the Yangtze River (~ between 30° N and 45° N), and the southern mode extending into the tropics (~ south of 30° N) (Figure 1b). Notably, a warmer climate typically coincides with a smaller area below a given temperature isoline, leading to observable negative correlations between temperature and the area below these isolines (Figure 2). Specifically, the northern mode exhibits significant negative correlations ($p < 0.1$) with temperatures across central and northeastern Asia (Figure 2a). For the central mode, these significant temperature correlations extend southward, impacting regions from

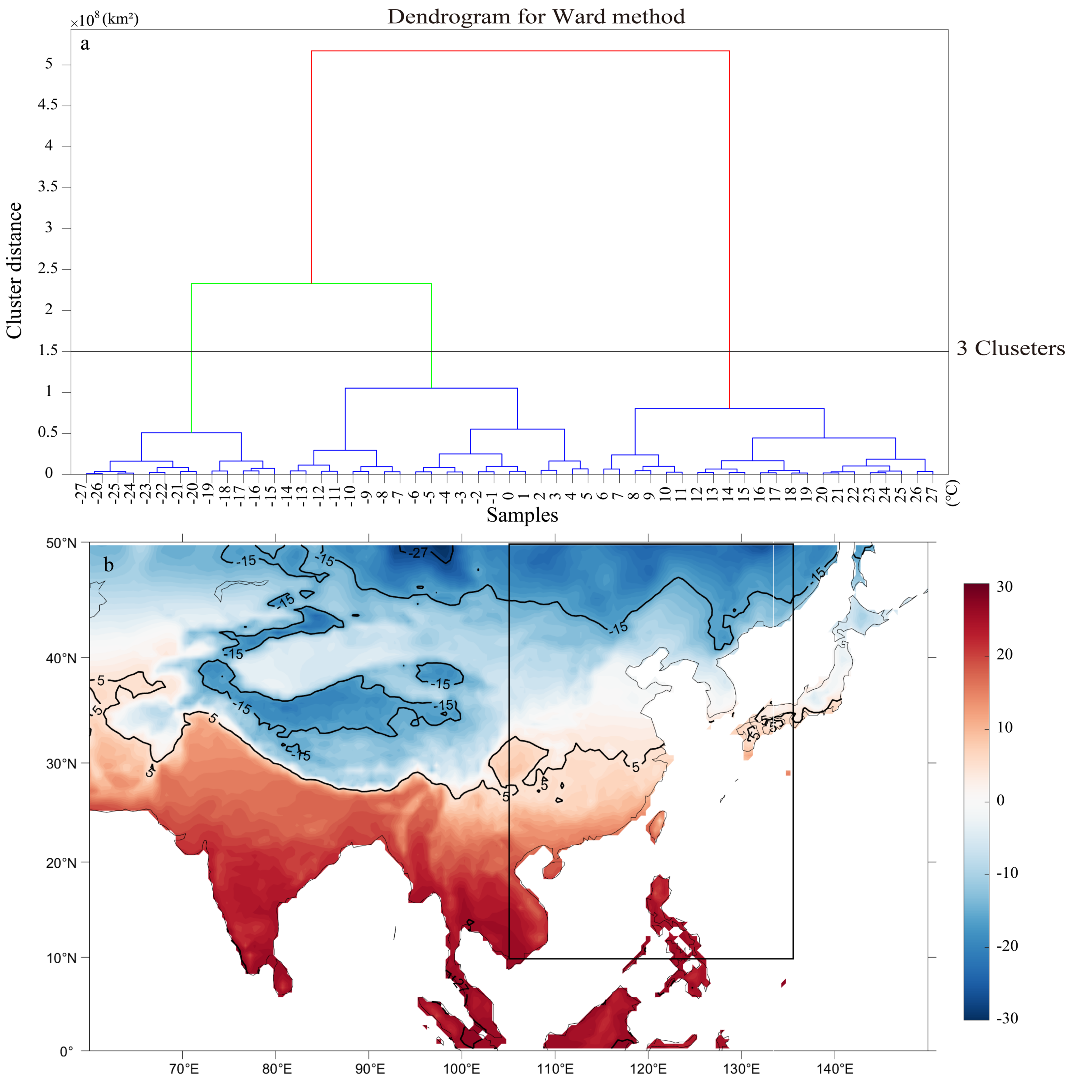

FIGURE 1 | Groupings of Winter (December–February) Temperature Isolines. (a) Classification tree for winter temperatures below specific isolines in eastern Asia. (b) The black square represents our calculation area, and the −15°C and −5°C temperature isolines divide eastern Asia into three regions, illustrating three distinct modes of the winter monsoon. [Colour figure can be viewed at wileyonlinelibrary.com]

central Asia to southeastern China (Figure 2b). The southern mode demonstrates strong temperature correlations along the southeastern Asian to eastern Chinese coastlines (Figure 2c). Compared to other EAWM indices, such as those defined by the sea-land pressure difference (Kim, Sohn, and Kug 2017), high-pressure characteristics (Zhi and Zheng 2022), low-level wind fields (Wang, Wu, and Wang 2022), and mid- to high-level wind fields (Zhu 2008) (Figure S1), our method demonstrates a stronger correlation with temperature (Figure 2).

The northern mode shows the weakest association with SST, with only weak correlations observed over the Indian Ocean (Figure 3a). In contrast, the central mode exhibits significant negative correlations ($p<0.1$) with SSTs, particularly over the western Pacific and Indian Ocean (Figure 3b). This pattern becomes even more pronounced in the southern mode (Figure 3c), where negative correlations extend further across the Indo-Pacific. This suggests that low-latitude oceanic patterns have a greater influence on EAWM temperatures in southern regions compared to northern areas. Conversely, the northern mode displays stronger correlations with Arctic atmospheric patterns than the central and southern modes (Figure 4) (Li et al. 2022; Sun, Li, and Zhou 2019; Sun et al. 2023). The positive correlations with low-troposphere (850 hPa) GPH predominantly occur over the Arctic (Figure 4a), aligning with the negative phase of the AO (Thompson and Wallace 1998). Negative correlations with the high GPH over high Asia are observed at the upper troposphere (200 hPa). The central and southern modes, however, exhibit weaker correlations with high-latitude GPH, instead showing stronger associations with GPH over the western Pacific and Indian Oceans (Figure 4c,f). Overall, the northern mode correlates strongly with atmospheric patterns linked to the AO, showing the highest correlation with the AO index ($r=-0.53$), while the central and southern modes exhibit weaker correlations, with coefficients of −0.39 and −0.14, respectively (Figure S2). Additionally, the central and southern modes correlate with SST and GPH along the eastern Asian and Indian Ocean coasts.

A warm northern mode correlates with enhanced westerlies over high Asia (Figure 5a) and weaker northerlies from the Arctic (Figure 5b). The influence of the westerlies on the EAWM

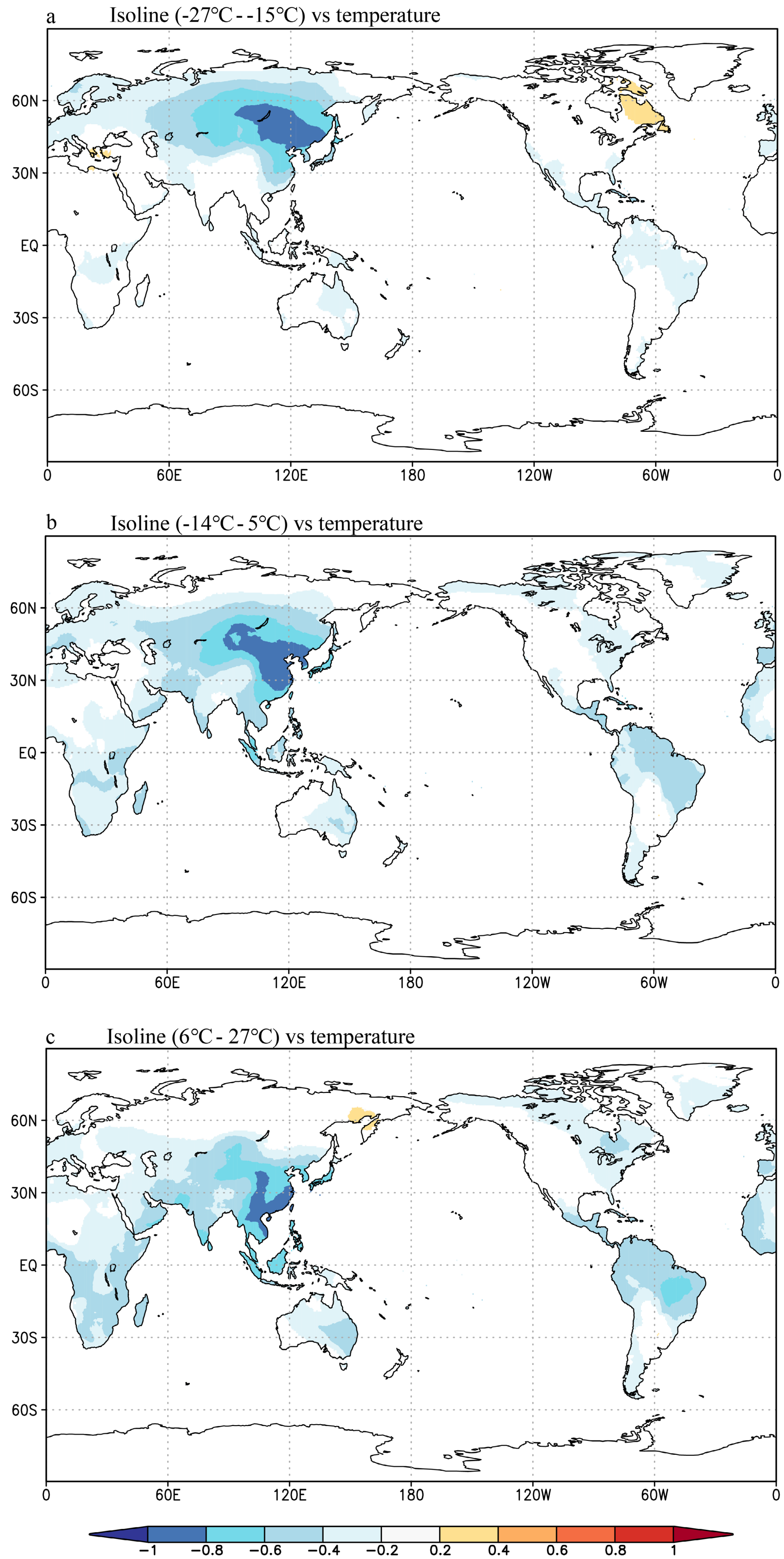

FIGURE 2 | Correlations between areas beneath winter (December–February) temperature isolines of (a) −27°C to −15°C, (b) −14°C to 5°C, and (c) 6°C to 27°C during the period 1950–2021. Maps only illustrate significant ($p < 0.1$) correlations. [Colour figure can be viewed at wileyonlinelibrary.com]

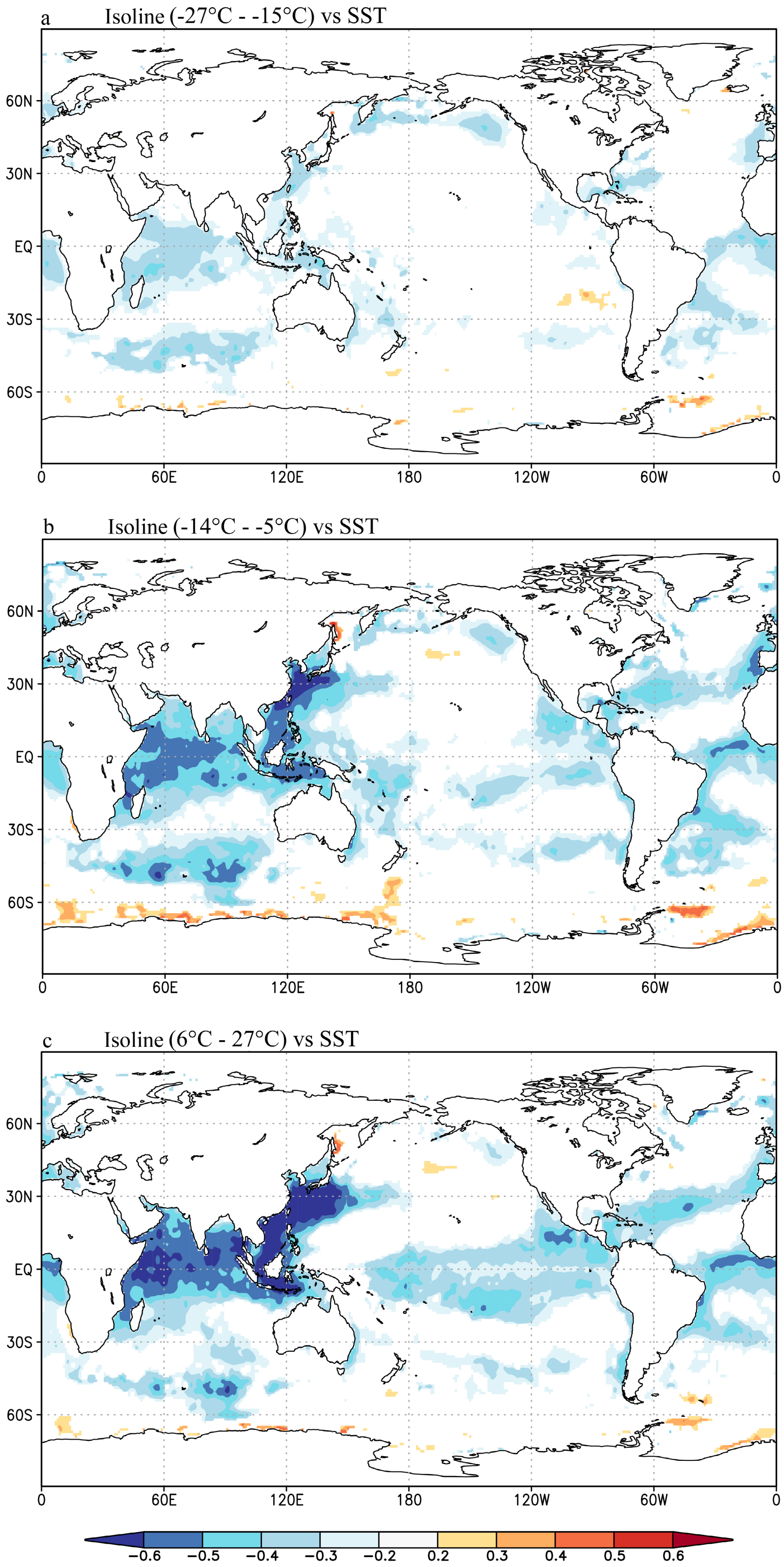

FIGURE 3 | Correlations of areas beneath winter (December–February) temperature isolines of (a) −27°C to −15°C, (b) −14°C to 5°C, and (c) 6°C to 27°C with the SST in winter (December–February) during the period 1950–2021. Only significant ($p < 0.1$) correlations are displayed. [Colour figure can be viewed at wileyonlinelibrary.com]

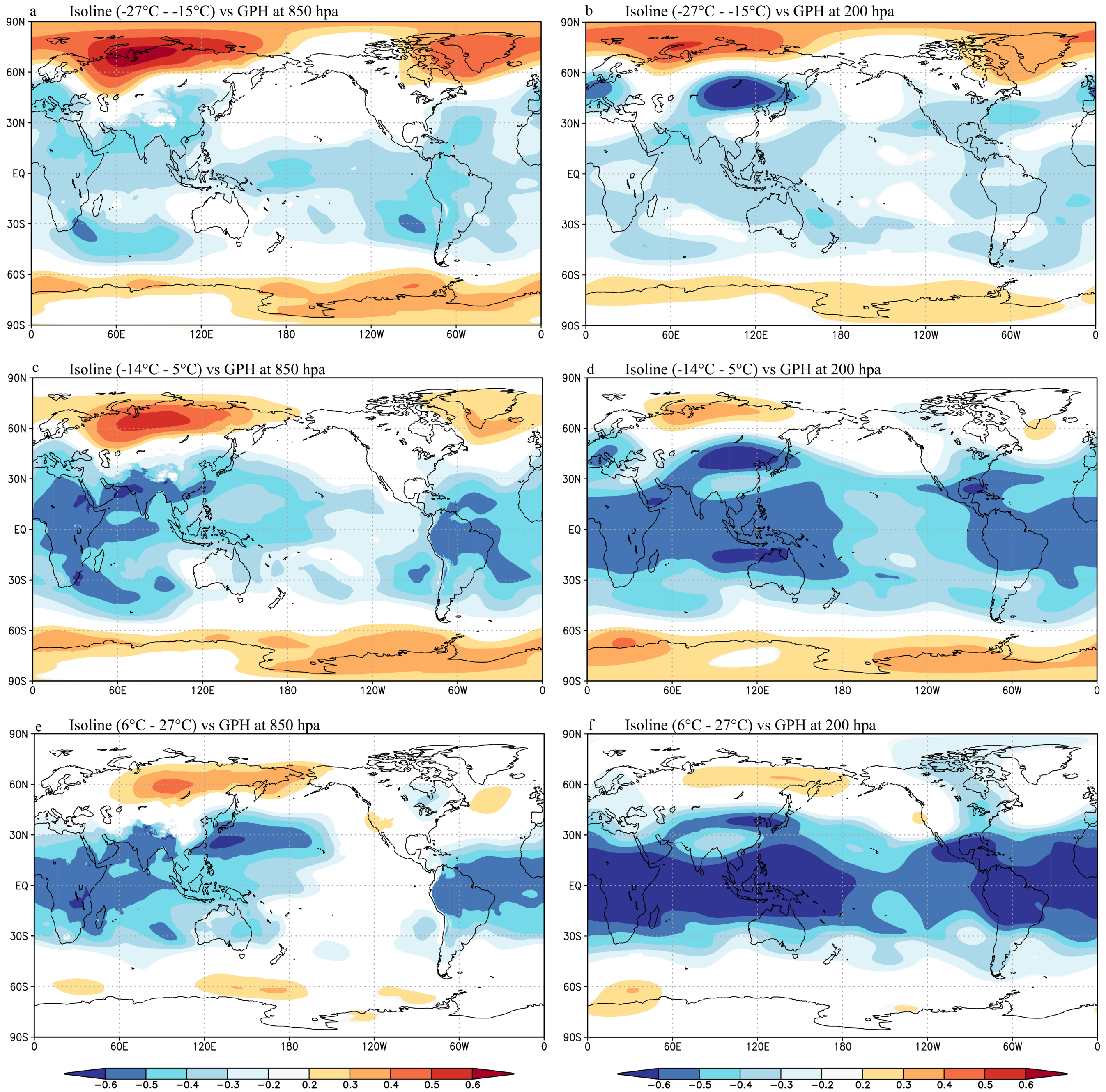

FIGURE 4 | Correlations of areas beneath winter (December–February) temperature isolines of (a and b) −27°C to −15°C, (c and d) −14°C to 5°C, and (e and f) 6°C to 27°C with geopotential height (GPH) at 850 hPa and 200 hPa during the period 1950–2021. Only significant ($p < 0.1$) correlations are displayed. [Colour figure can be viewed at wileyonlinelibrary.com]

diminishes for the central and southern modes (Figure 5c,e), which instead show strong correlations with northerlies near the eastern Asian coast, particularly in the southern mode (Figure 5f). This indicates the significant role of tropical and subtropical southerlies in shaping the EAWM.

Post-1990, correlations between the areas of the northern and central modes have strengthened, particularly at interannual timescales (Figure 6a,b). Conversely, correlations between the central and southern modes have weakened, especially after 1990, and predominantly at interannual timescales (Figure 6c,d). The low correlation between the northern and southern modes is attributed to their modulation by high- and low-latitude drivers, respectively. The declining trend post-1980s and the evolving correlation patterns around 1990 suggest a potential shift in the EAWM regime around that time.

All areas of the northern, central, and southern modes exhibit a declining trend, coinciding with global warming reducing areas below given temperature isolines (Figure 6). This downtrend is especially pronounced around the 1980s, corroborating earlier studies (He 2013; Ma and Chen 2021; Yu, Zhang, and Zhong 2019). Post-1990, correlations between the northern and central modes have strengthened, particularly at interannual timescales (Figure 6a,b). Conversely, correlations between the central and southern modes have weakened, especially after

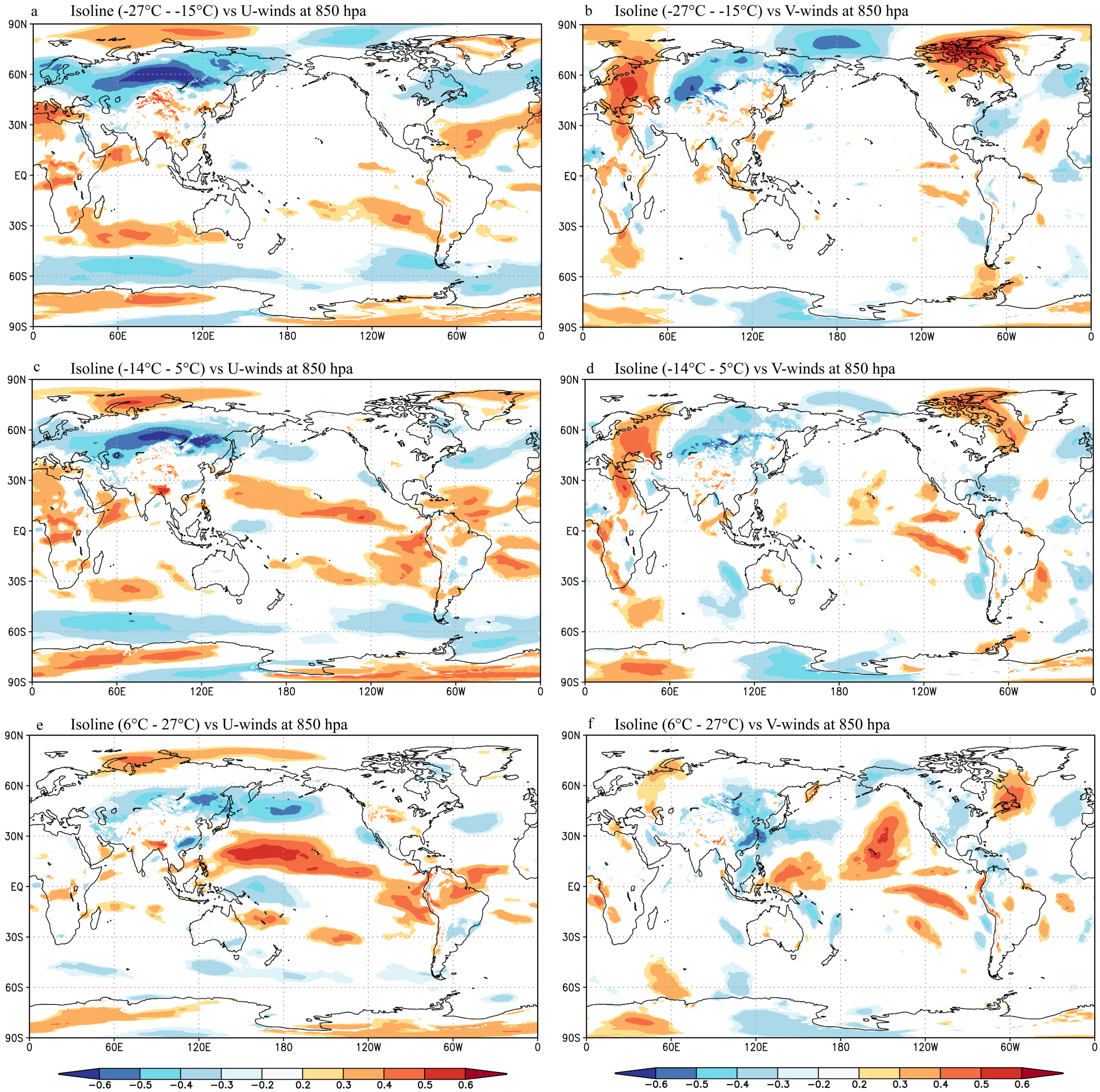

FIGURE 5 | Correlations of areas beneath winter (December–February) temperature isolines of (a and b) −27°C to −15°C, (c and d) −14°C to 5°C, and (e and f) 6°C to 27°C with zonal (U) and meridional (V) wind fields at 850 hPa during the period 1950–2021. Only significant ($p < 0.1$) correlations are displayed. [Colour figure can be viewed at wileyonlinelibrary.com]

1990 at interannual timescales (Figure 6c,d). The declining trend post-1980s and the evolving correlation patterns around 1990 suggest a potential shift in the EAWM regime around that time.

The EAWM exhibits time-varying relationships with GPH before and after 1990 (Figure 7). Prior to 1990, all three modes (northern, central, and southern) displayed stronger correlations with high Asia GPH, indicative of significant high-latitude atmospheric pattern impacts (Figure 7a,c,e). However, after 1990, the influence of the positive geopotential height over the high latitudes of Eurasia on the southern mode weakened. In contrast, low-latitude drivers had a significantly stronger impact on the southern, central, and northern modes (Figure 7b,d,f), as evidenced by the spatial correlation analysis with SST (Figure S3), zonal wind fields (Figure S4), and meridional wind (Figure S5).

4 | Discussion

In this study, we grouped EAWM temperatures into three groups, defined by the area below specific temperature thresholds. This approach, based on the concept that covarying isolines indicate control by similar circulation patterns, offers an innovative perspective on EAWM dynamics. Traditional climate classifications typically rely on the co-variability of

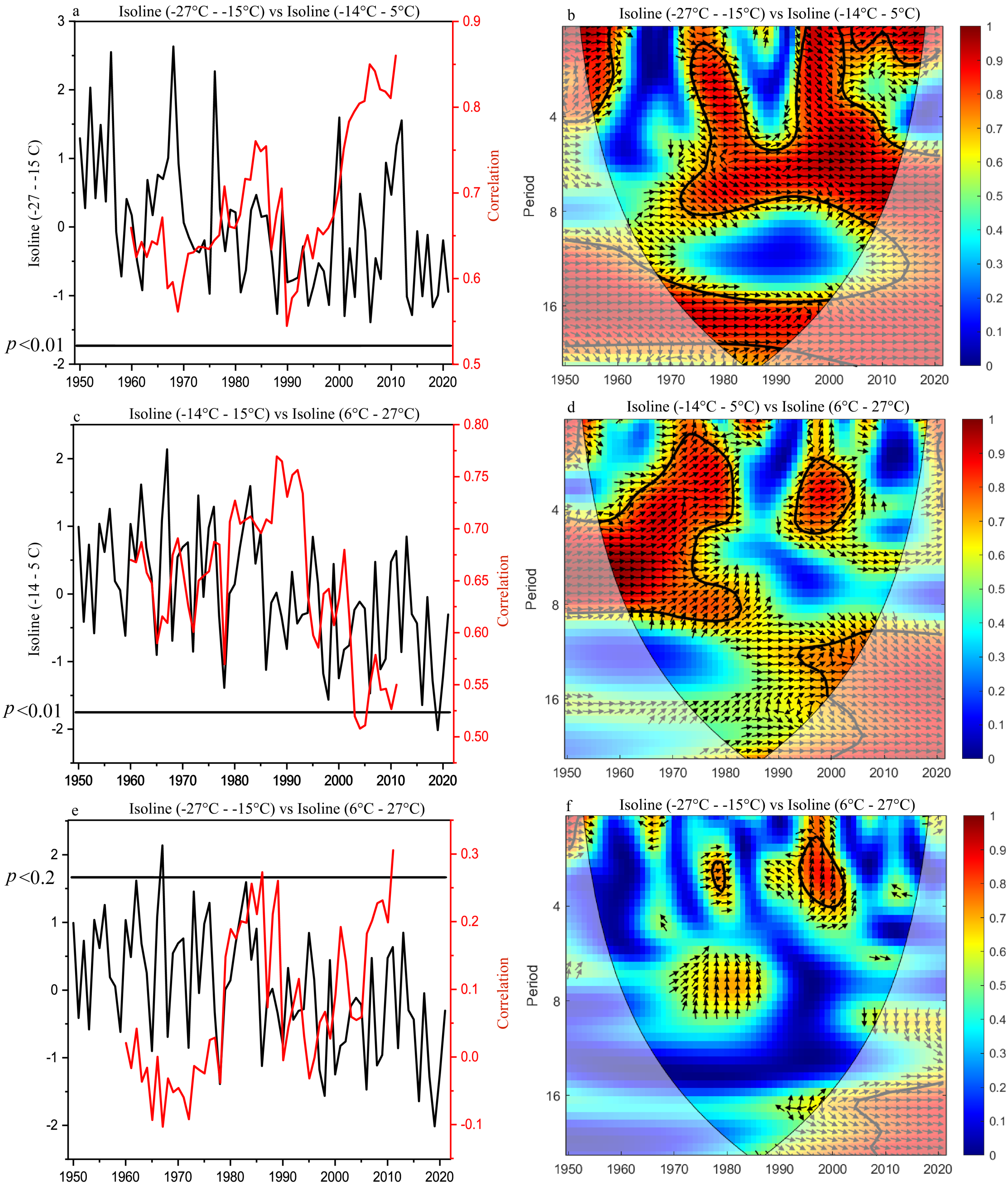

FIGURE 6 | Interplay among winter (December–February) temperature below various isolines. (a) The temperatures below the −27°C to −15°C isoline, their running (21-year window) correlations with temperatures below the −14°C to 5°C isoline, and (b) their wavelet coherence (WTC); (c) temperatures below the −14°C to 5°C isoline, their running correlations with temperatures below the 6°C to 27°C isoline, and (d) their WTC; (e) temperatures below the 6°C to 27°C isoline, their running correlations with temperatures below the −27°C to −15°C isoline, and (f) their WTC. The black line segment in the left panel indicates the significance threshold for the correlation. [Colour figure can be viewed at wileyonlinelibrary.com]

regional climate time series (Lorenz 1956), often overlooking the absolute climate conditions (Fang et al. 2018, 2014). The methodology adopted is grounded in temperature isolines, combining both aspects: the co-variability of regional climate changes and their absolute climatic conditions. Consequently, this temperature isoline method provides a more nuanced representation of

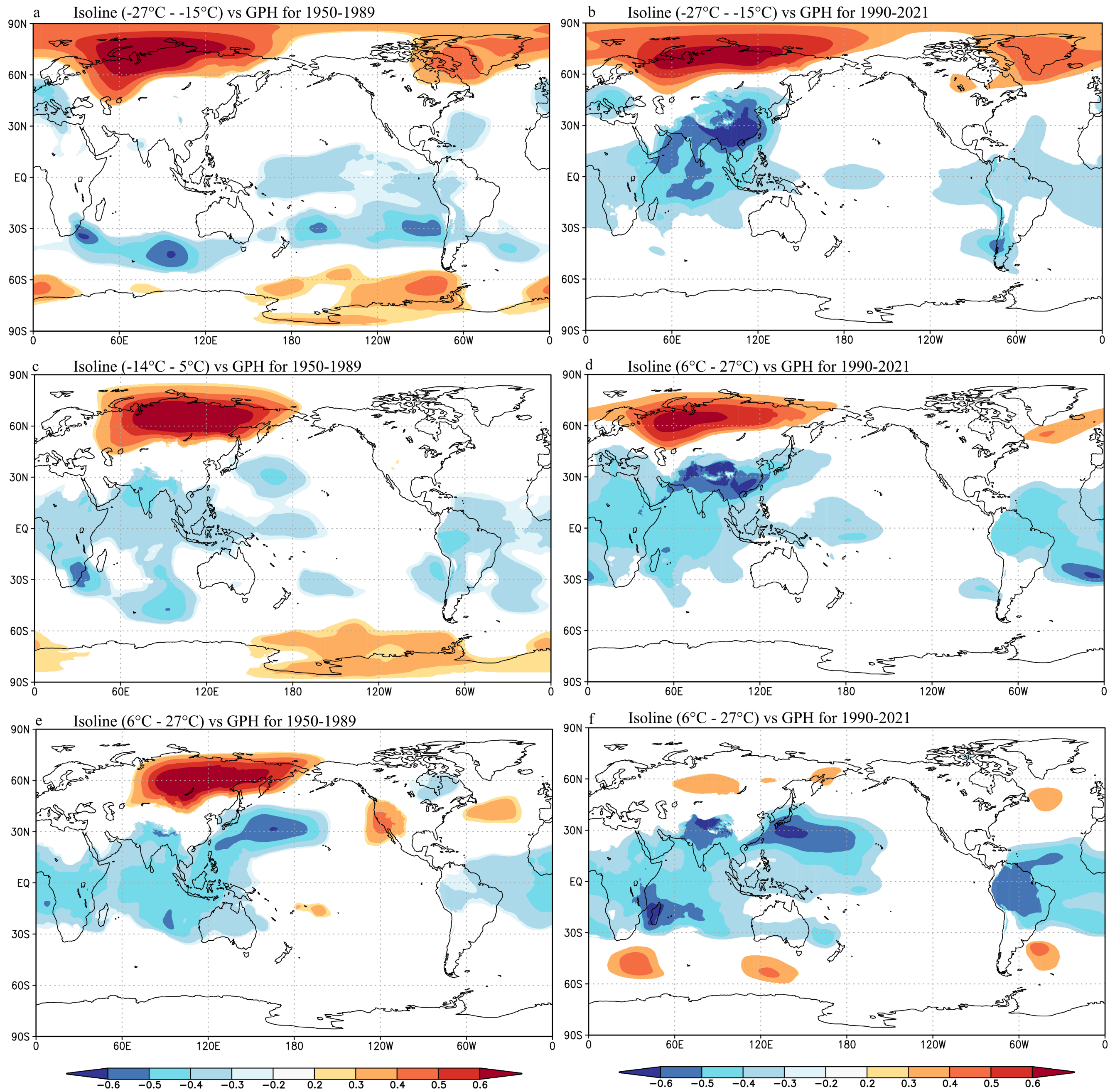

FIGURE 7 | Correlations of areas beneath winter (December–February) temperature isolines of (a and b) −27°C to −15°C, (c and d) −14°C to 5°C, and (e and f) 6°C to 27°C with the geopotential height (GPH) across two intervals, 1950–1989 and 1990–2021. Only significant ($p < 0.1$) correlations are displayed. [Colour figure can be viewed at wileyonlinelibrary.com]

the spatial shifts in temperature patterns affected by EAWM (Fang et al. 2024).

The dichotomy in temperature patterns between the northern and southern domains of the EAWM is well-established (Ma and Chen 2021). Our findings describe the boundaries of the northern, central, and southern modes associated with EAWM temperature changes. While the northern and southern modes are dominated by high- and low-latitude drivers, respectively, neither mode exhibits simultaneous connections to both high- and low-latitude atmospheric and oceanic patterns. We suggest that the central mode, bridging both high- and low-latitude influences, may better represent the overarching characteristics of the EAWM. This mode predominantly reflects areas north of the winter temperature isoline of 5°C, aligning with key geographical regions like the southern Himalayan Mountains and the Yangtze River (Figure 1b). Despite the EAWM's marginal impact on tropical regions, it predominantly governs winter temperatures north of the 5°C isoline (Wang and Lu 2017).

The EAWM indices derived from our winter temperature analysis generally resonate well with the atmospheric patterns described by previous indices (Wang and Chen 2010). However, a notable distinction is our indices' weaker correlations with the low-troposphere Siberian-Mongolian High, compared to previous indices (Jhun and Lee 2004; Wang et al. 2006; L. Wang and Chen 2010), as demonstrated in Figure 4a. This discrepancy arises because the Siberian-Mongolian High typically triggers cold surges in a northwest-southeast direction, diverging from our zonally distributed temperature isoline-based indices (Figure 1b). Our indices instead show robust correlations with zonally elongated westerlies and the AO. Particularly over the high troposphere, our indices correlate strongly with the Siberian-Mongolian High (Figure 4b), reflecting less sensitivity to regional surface temperature patterns than its low-troposphere counterpart. Our approach effectively captures the regime where enhanced westerlies during the AO's positive phase constrain the Arctic cold air mass, leading to a weakened EAWM (Fan and Wang 2006; Fang et al. 2022; Gong, Wang, and Zhu 2001).

The amplified influence of low-latitude processes on the EAWM since around 1990 might be linked to the interdecadal weakening of the EAWM in the late 1980s (He 2013; Yancheva et al. 2007), the interdecadal variation in Siberian High intensity (Jeong et al. 2011) and the reduced winter snow in the 1990s (Ma and Chen 2021). The low-latitude factors impacting the EAWM are predominantly associated with western Pacific SST and the consequent intensification of the Western Pacific branch of the Hadley Circulation (Ma and Chen 2021). Generally, the Hadley Circulation has expanded and shifted poleward in response to the current warming trend (Fu et al. 2006; Seidel et al. 2007). The western Pacific, experiencing one of the most pronounced SST warming trends (Cravatte et al. 2009), may exhibit an anomalously enhanced Western Pacific Hadley Circulation. This northward shift of the Hadley Circulation could be a key factor in the rising influence of low-latitude processes on the EAWM (Figure S5).

5 | Conclusions

In this study, we delineated the northern (below −27°C to −15°C), central (below −14°C to 5°C), and southern (below 4°C to 27°C) modes of winter temperatures within the EAWM domain, employing a novel approach centred on the co-variability of areas lower than varying temperature thresholds. Our analysis reveals that the central mode, with its connections to both high- and low-latitude oceanic and atmospheric processes, most comprehensively encapsulates the EAWM's overall characteristics. This method, based on temperature isolines, demonstrates enhanced correlations with zonally distributed atmospheric patterns, offering a more refined perspective compared to previous indices.

A key finding of our research is the strong correlation between the EAWM and zonally elongated atmospheric patterns, including enhanced westerlies and the positive phase of the AO. These dynamics play a crucial role in trapping the Arctic cold air mass, leading to a weakened EAWM. In the context of global warming, the pronounced warming of the western Pacific Ocean and the resultant intensification of the Western Pacific Hadley Circulation have emerged as significant factors. This phenomenon appears to amplify the influence of low-latitude processes on the EAWM, particularly post-1990. Our study underscores the evolving nature of the EAWM, highlighting the increasing importance of low-latitude dynamics in the face of ongoing global climate changes.

Author Contributions

Bozhou Chen: writing – original draft, writing – review and editing, formal analysis, software. **Keyan Fang:** software, methodology, validation, conceptualization, investigation. **Zepeng Mei:** software, formal analysis, methodology, writing – review and editing. **Tinghai Ou:** writing – review and editing, software, formal analysis, methodology. **Feifei Zhou:** methodology, software, formal analysis. **Hao Wu:** methodology, software, formal analysis. **Zheng Zhao:** methodology, software, formal analysis. **Deliang Chen:** methodology, software, formal analysis, writing – review and editing.

Acknowledgements

This study was supported by the National Natural Science Foundation of China (42101082 and 42130507), China Postdoctoral Science Foundation (2023M730602).

Conflicts of Interest

The authors declare no conflicts of interest.

Data Availability Statement

The data that support the findings of this study are available from the corresponding author upon reasonable request.

References

Ao, K., X. Geng, W. Zhang, and L. Wang. 2024. "Comparative Analysis of the Performance of East Asian Winter Monsoon Indices in Capturing Winter Climate Change Over China." *Acta Meteorologica Sinica* 82, no. 2: 168–189.

Cook, E., K. J. Anchukaitis, B. M. Buckley, R. D. D'Arrigo, G. C. Jacoby, and W. E. Wright. 2010. "Asian Monsoon Failure and Megadrought During the Last Millennium." *Science* 328: 486–489.

Cravatte, S., T. Delcroix, D. Zhang, M. McPhaden, and J. Leloup. 2009. "Observed Freshening and Warming of the Western Pacific Warm Pool." *Climate Dynamics* 33: 565–589.

Duan, J., Q. Zhang, and L. X. Lv. 2013. "Increased Variability in Cold-Season Temperature Since the 1930s in Subtropical China." *Journal of Climate* 26, no. 13: 4749–4757.

Fan, K., and H. Wang. 2006. "Interannual Variability of Antarctic Oscillation and Its Influence on East Asian Climate During Boreal Winter and Spring." *Science in China* 49, no. 5: 554–560.

Fang, K., M. Bai, C. Azorin-Molina, et al. 2022. "Wind Speed Reconstruction From a Tree-Ring Difference Index in Northeastern Inner Mongolia." *Dendrochronologia* 72: 125938.

Fang, K., E. Cook, Z. Guo, et al. 2018. "Synchronous Multi-Decadal Tree-Ring Patterns of the Pacific Areas Reveal Dynamics of the Interdecadal Pacific Oscillation (IPO) Since 1567." *Environmental Research Letters* 13: 024016. https://doi.org/10.1088/1748-9326/aa9f74.

Fang, K., H. Seppä, J. Morris, S. Salonen, and J. Li. 2014. "Covarying Hydroclimate Patterns Between Monsoonal Asia and North America Over the Past 600 Years." *Journal of Climate* 27: 8017–8033.

Fang, K., Z. Mei, S. Lin, et al. 2024. *Warming Driven Expansions of the co-varying Global Monsoon Margins*. Under review.

Fu, Q., C. M. Johanson, J. M. Wallace, and T. Reichler. 2006. "Enhanced Mid-Latitude Tropospheric Warming in Satellite Measurements." *Science* 312, no. 5777: 1179.

Gong, D. Y., S. W. Wang, and J. H. Zhu. 2001. "East Asian Winter Monsoon and Arctic Oscillation." *Geophysical Research Letters* 28, no. 10: 2073–2076.

Grinsted, A., J. C. Moore, and S. Jevrejeva. 2004. "Application of the Cross Wavelet Transform and Wavelet Coherence to Geophysical Time Series." *Nonlinear Processes in Geophysics* 11, no. 5/6: 561–566.

Harris, I., T. J. Osborn, P. Jones, and D. Lister. 2020. "Version 4 of the CRU TS Monthly High-Resolution Gridded Multivariate Climate Dataset." *Scientific Data* 7, no. 1: 109.

He, S. 2013. "Reduction of the East Asian Winter Monsoon Interannual Variability After the Mid-1980s and Possible Cause." *Chinese Science Bulletin* 58: 1331–1338.

Hersbach, H., B. Bell, P. Berrisford, G. Biavati, A. Horányi, and J. M. Sabater. 2023. ERA5 Hourly Data on Single Levels From 1940 to Present. Copernicus Climate Change Service (C3S) Climate Data Store (CDS).

Huang, L., J. Chen, K. Yang, et al. 2023. "The Northern Boundary of the Asian Summer Monsoon and Division of Westerlies and Monsoon Regimes Over the Tibetan Plateau in Present-Day." *Science China Earth Sciences* 66, no. 4: 882–893.

Huang, W., B. Wang, and J. S. Wright. 2016. "A Potential Vorticity-Based Index for the East Asian Winter Monsoon." *Journal of Geophysical Research-Atmospheres* 121: 9382–9399. https://doi.org/10.1002/2016JD025053.

Jeong, J. H., T. Ou, H. W. Linderholm, et al. 2011. "Recent Recovery of the Siberian High Intensity." *Journal of Geophysical Research: Atmospheres* 116: D23102.

Jhun, J.-G., and E.-J. Lee. 2004. "A New East Asian Winter Monsoon Index and Associated Characteristics of the Winter Monsoon." *Journal of Climate* 17, no. 4: 711–726.

Jin, C., B. Wang, J. Liu, L. Ning, and M. Yan. 2019. "Decadal Variability of Northern Asian Winter Monsoon Shaped by the 11-Year Solar Cycle." *Climate Dynamics* 53: 6559–6568.

Kim, S. T., S.-J. Sohn, and J.-S. Kug. 2017. "Winter Temperatures Over the Korean Peninsula and East Asia: Development of a New Index and Its Application to Seasonal Forecast." *Climate Dynamics* 49, no. 5: 1567–1581.

Lee, S.-S., S.-H. Kim, J.-G. Jhun, K.-J. Ha, and Y.-W. Seo. 2013. "Robust Warming Over East Asia During the Boreal Winter Monsoon and Its Possible Causes." *Environmental Research Letters* 8, no. 3: 034001.

Li, H., B. Sun, H. Wang, B. Zhou, and M. Duan. 2022. "Mechanisms and Physical-Empirical Prediction Model of Concurrent Heatwaves and Droughts in July–August Over Northeastern China." *Journal of Hydrology* 614: 128535.

Li, H., B. Sun, H. Wang, B. Zhou, and X. Ma. 2023. "Characteristics and Mechanisms of the Severe Compound Cold-Wet Event in Southern China During February 2022." *Environmental Research Letters* 18, no. 11: 114021.

Li, Y., and S. Yang. 2010. "A Dynamical Index for the East Asian Winter Monsoon." *Journal of Climate* 23, no. 15: 4255–4262.

Liu, G., L.-R. Ji, S.-Q. Sun, and Y.-F. Xin. 2012. "Low-and Mid-High Latitude Components of the East Asian Winter Monsoon and Their Reflecting Variations in Winter Climate Over Eastern China." *Atmospheric and Oceanic Science Letters* 5, no. 3: 195–200.

Lorenz, E. N. 1956. *Empirical Orthogonal Functions and Statistical Weather Prediction*. Vol. 1. Cambridge, MA: Massachusetts Institute of Technology, Department of Meteorology Cambridge.

Ma, T., and W. Chen. 2021. "Climate Variability of the East Asian Winter Monsoon and Associated Extratropical–Tropical Interaction: A Review." *Annals of the New York Academy of Sciences* 1504, no. 1: 44–62.

Rayner, N. A., D. E. Parker, E. B. Horton, et al. 2003. "Global Analyses of Sea Surface Temperature, Sea Ice, and Night Marine Air Temperature Since the Late Nineteenth Century." *Journal of Geophysical Research* 108, no. D14: 4407.

Seidel, D. J., Q. Fu, W. J. RanDel, and T. S. J. ReichleR. 2007. "Widening of the Tropical Belt in a Changing Climate." *Nature Geoscience* 1, no. 1: 21–24.

Snyder, J. P. 1987. *Map Projections–A Working Manual*. Washington D.C: US Geological Survey Professional Paper.

Sun, B., H. Li, and B. Zhou. 2019. "Interdecadal Variation of Indian Ocean Basin Mode and the Impact on Asian Summer Climate." *Geophysical Research Letters* 46, no. 21: 12388–12397.

Sun, B., H. Li, B. Zhu, R. Xue, and W. Li. 2023. "Sources of the Predictability of Month-to-Month Variation of Precipitation Anomalies in East Asia During Summer." *International Journal of Climatology* 43, no. 15: 7274–7291.

Tao, S. Y., and J. Wei. 2008. "Severe Snow and Freezing-Rain in January 2008 in the Southern China." *Climatic and Environmental Research* 13, no. 4: 337–350.

Thompson, D. W. J., and J. M. Wallace. 1998. "The Arctic Oscillation Signature in the Wintertime Geopotential Height and Temperature Fields." *Geophysical Research Letters* 25, no. 9: 1297–1300.

Wang, B., C.-P. Chang, Z. Wang, and H. Hendon. 2006. "The Asian Winter Monsoon." *Asian Monsoon* 3: 89–127.

Wang, B., J. Liu, H.-J. Kim, P. J. Webster, S.-Y. Yim, and B. Xiang. 2013. "Northern Hemisphere Summer Monsoon Intensified by Mega-El Niño/Southern Oscillation and Atlantic Multidecadal Oscillation." *Proceedings of the National Academy of Sciences* 110, no. 14: 5347–5352.

Wang, L., and W. Chen. 2010. "How Well Do Existing Indices Measure the Strength of the East Asian Winter Monsoon?" *Advances in Atmospheric Sciences* 27: 855–870.

Wang, L., and M. M. Lu. 2017. "The East Asian Winter Monsoon." In *The Global Monsoon System: Research and Forecast*. Singapore: World Scientific.

Wang, Z., R. Wu, and Y. Wang. 2022. "Impacts of the East Asian Winter Monsoon on Winter Precipitation Variability Over East Asia-Western North Pacific." *Climate Dynamics* 58, no. 11: 3041–3055.

Ward, J. H. 1963. "Hierarchical Grouping to Optimize an Objective Function." *Journal of the American Statistical Association* 58, no. 301: 236–244.

Yancheva, G., N. R. Nowaczyk, J. Mingram, et al. 2007. "Influence of the Intertropical Convergence Zone on the East Asian Monsoon." *Nature* 445, no. 7123: 74–77.

Yang, S., K. Lau, and K. Kim. 2002. "Variations of the East Asian Jet Stream and Asian–Pacific–American Winter Climate Anomalies." *Journal of Climate* 15, no. 3: 306–325.

Yu, P., L. Zhang, and Q. Zhong. 2019. "Contrasting Relationship Between the Kuroshio Extension and the East Asian Summer Monsoon Before and After the Late 1980s." *Climate Dynamics* 52: 929–950.

Yu, Y., Y. Li, R. Ren, M. Cai, Z. Guan, and W. Huang. 2022. "An Isentropic Mass Circulation View on the Extreme Cold Events in the 2020/21 Winter." *Advances in Atmospheric Sciences* 39, no. 4: 643–657.

Zhi, R., and Z. Zheng. 2022. "Characteristics of Climate Anomalies Over China in Winter 2021/2022 and Causes for Precipitation Anomalies Over Southern China." *Meteorological Monthly* 48, no. 7: 925–935.

Zhu, Y. 2008. "An Index of East Asian Winter Monsoon Aplied to Description the Chinese Mainland Winter Temperature Changes." *Acta Meteorologica Sinica* 3: 781–788.

Supporting Information

Additional supporting information can be found online in the Supporting Information section.